A Rheo-Optical Study on Polystyrene under Large Tensile Deformation around the Glass Transition Temperature

Tadashi Inoue,* Deug-Soo Ryu, and Kunihiro Osaki

Institute for Chemical Research, Kyoto University, Uji, Kyoto 611, Japan

Received June 23, 1997; Revised Manuscript Received December 15, 1997

ABSTRACT: The tensile stress and the birefringence of polystyrene were measured under elongation at a constant rate up to the elongation ratio of 4 at 115, 105, and 100 °C. The tensile stress was separated into two component functions, designated with subscripts R and G, through a modified stress−optical rule, MSOR, considering the effect of finite extensibility of the polymer chain on the stress dependence of the stress-optical coefficient. The R component represents the stress attributed to the polymer segment orientation and the G component to the twist of the polymer chain. At 115 °C, the time dependence of the viscosity growth function of the two components, η_{ER}^+ and η_{EG}^+, can be described in the framework of linear viscoelasticity except for a steep increase of η_{ER}^+ at times longer than $1/(2\dot{\epsilon})$, where $\dot{\epsilon}$ is the rate of elongation. It is well-known that this type of steep increase is due to the strong increase of strain measured under elongation at a constant rate. At lower temperatures, η_{EG}^+ decreased with increasing strain rate when the rate exceeds $^1/_{1000}$ of the characteristic relaxation rate of the G component. The steady value of the elongational viscosity, $\eta_{EG}(\dot{\epsilon})$, at various temperatures supported a master curve when $\eta_{EG}(\dot{\epsilon})/\eta_{EG}(0)$ is plotted against $\dot{\epsilon}\, a_{TG}$, where a_{TG} is the shift factor for the G component determined in dynamic viscoelastic measurements. On the other hand, η_{ER}^+ is always close to the linear viscoelasticity except for the steep rise at $t > 1/(2\dot{\epsilon})$. The relaxation rate of the R component was enhanced in proportion to $\eta_{EG}(0)/\eta_{EG}(\dot{\epsilon})$ when the G component showed thinning. Thus, MSOR analysis simplifies the complicated nonlinear viscoelastic response of amorphous polymers around the glass transition temperature.

Introduction

When a polymeric material is deformed, birefringence arises as well as stress. The relation between birefringence and stress has long been a subject of rheo-optical studies. For polymer melts and concentrated solutions, the anisotropic part of the refractive index tensor, $\mathbf{n}(t)$, is proportional to that of the stress tensor, $\sigma(t)$.[1] This empirical rule is called the stress−optical rule, SOR. The SOR for tensile deformation can be written as follows.

$$\Delta n(t) = C\sigma(t) \tag{1}$$

Here, $\Delta n(t)$ is the birefringence and $\sigma(t)$ is the tensile stress. The coefficient of proportionality, C, is called the stress−optical coefficient.

The validity of the rule has been examined for many polymeric systems. From a theoretical point of view, the SOR indicates that the molecular origin of the stress as well as the birefringence is attributed to the orientation of the chain. Many molecular theories can predict the validity of the rule in rubbery or liquid states.[2,3]

However, the validity of the SOR is limited for two experimental conditions even if the system is a neat polymer melt. First, the SOR is not valid at high stress levels due to the finite extensibility of the chain. In the case of polystyrene, the linear stress−optical relation fails if the tensile stress exceeds 2 MPa.[4] Second, when the temperature of the system is close to the glass transition temperature, T_g, the SOR becomes invalid. The glassy component of the stress, the molecular origin of which is not the orientation of flexible chains, contributes to both the stress and the birefringence.

* To whom all correspondence should be addressed.

The contribution of the glassy stress can be quantitatively described with a modified stress−optical rule, MSOR.[5] The MSOR assumes that both the stress and the birefringence are composed of two component functions and that a rule similar to the ordinary SOR holds well for each component function. The MSOR for tensile deformation can be written as follows.

$$\sigma(t) = \sigma_R(t) + \sigma_G(t) \tag{2}$$

$$\Delta n(t) = C_R\sigma_R(t) + C_G\sigma_G(t) \tag{3}$$

Here, $\sigma_i(t)$ is the ith component function (i = R or G) of the stress and C_i is the stress−optical coefficient for the ith component function. C_i may be regarded as independent of temperature. The validity of the MSOR has been confirmed on many polymeric systems.[6]

A molecular interpretation of the MSOR was proposed by Osaki et al.[6] The R component is attributed to the orientation of flexible chains since at high temperatures or with long times the terms with the subscript G disappear and the MSOR is reduced to the ordinary stress−optical rule. On the other hand, the relaxation of the G component can be attributed to the rotational reorientation of structure units about the main chain axis.[7,8]

The MSOR was applied to large tensile deformations of amorphous polymers by Okamoto et al.[9,10] They measured the tensile stress and the birefringence of polystyrene and polycarbonate under constant-speed elongation and applied the MSOR assuming that the two stress−optical coefficients are independent of the stress level, which is obviously unsatisfactory at high stresses. Their result is not accurate for high stresses, but they succeeded in showing that strong nonlinear features such as yield phenomena or plasticity observed

S0024-9297(97)00908-X CCC: $15.00
Published on Web 09/17/1998

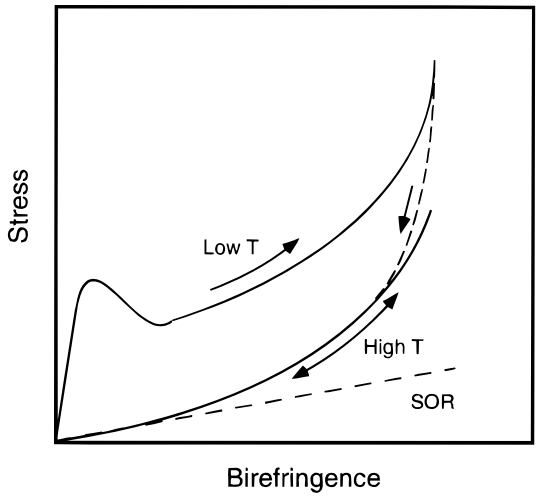

Figure 1. Schematic diagram of the stress−birefringence relation.

near T_g could be attributed to the strong nonlinear viscoelasticity of the G component. On the other hand, the behavior of the R component was found to be close to that predicted with linear viscoelasticity.

Muller and Pesce studied stress−optical behavior of polystyrene and polycarbonate more in detail by performing constant-rate elongation experiments near the glass transition temperature.[11] A schematic graph of their results is presented in Figure 1, in which the tensile stress is plotted against the birefringence. At high temperatures, the SOR holds well if the stress level is low, and the stress−birefringence curve starts to deviate from the linear SOR at high stresses. This deviation can be qualitatively explained by a finite chain extensibility that results in a saturation of the orientation and hence of the birefringence.[12] Near T_g, the simple SOR does not hold even at low stresses at the beginning of deformation. However, in the relaxation process after elongation, the stress−optical relation can be described by a single curve except at the very early stage of relaxation. The relaxation curves under various conditions of elongation ratio, elongation rate, or temperature form a common curve after short relaxation times. The curve agrees with the stress−birefringence relaxation at high temperatures, including the processes of elongation and relaxation. They named this curve the equilibrium curve. Their result indicates that C_R should be stress-dependent.

The aim of the present work is to investigate the viscoelastic properties of the two component functions in detail, taking into account the stress dependence of C_R. For this purpose, we perform constant-rate elongation experiments with polystyrene. The tensile stress is separated into the two component functions, and effects of the elongation rate on them at 115, 105, and 100 °C are discussed.

Experimental Section

Material. Polystyrene (Toporex 550-51) was supplied by Mitsui-Toatsu Co. Ltd. GPC measurement showed the polymer to have a molecular weight (M_w) of 270 000 and a polydispersity index of 2.1. The results of dynamic viscoelasticity and birefringence measurements were reported previously.[14] The two MSOR component functions for the complex Young's modulus and shift factors for them are also included in the same reference. T_g (102 °C) was measured with DSC (TA Instrument, thermal analysis system 2000 with DSC 2910) by the midpoint method. After being held at 200 °C for 2 min, the sample was cooled at 10 K/min to 50 °C, held there for 2 min, and then heated with a heating rate of 10 K/min. The sample was molded into a plate with a 0.5 mm thickness at 200 °C. Dumbbell-shaped specimens were cut out from this plate.

Apparatus. The stress−optical behavior in uniaxial extension with constant elongation rates was examined with a tensile tester (Creepmeter RE-33005, Yamaden Co Ltd., Tokyo, Japan) equipped with a simple optical system for birefringence measurements. In this study, the apparatus was modified to perform constant-rate experiments. A signal generator (1941, NF Electric Instrument Co., Yokohama, Japan) was used to vary the pulse interval to drive the pulse motor to achieve an exponentially increasing elongation ratio. The elongation ratio, λ, is related to the rate of elongation $\dot{\epsilon}$, as follows

$$\lambda = \exp(\epsilon) \tag{4}$$

$$\epsilon = \dot{\epsilon}t \tag{5}$$

Here, ϵ is the Hencky strain. The uniformity of elongation was checked by examining the films at various draw ratios. The uniformity was satisfactory in the ranges of temperature and rate of elongation of this study.

The optical system for birefringence measurements was based on the intensity method. Details of the optical system were the same as described previously.[9,13] A homemade chamber was used to control the temperature of the sample. The temperature of the sample was calibrated by using the melting point of indium (T_m = 156.6 °C).

In evaluating the stress and the birefringence from the directly detected quantities, the tensile force and the retardation, respectively, one needs the exact cross sectional area and thickness of the specimen. We estimated the cross sectional area from the initial cross sectional area assuming that the material is incompressible or that the Poisson ratio is equal to 0.5. The Poisson ratio for glassy polystyrene is reported to be 0.33. We expect that the Poisson ratio at temperatures higher than T_g is larger than 0.33 and that the error due to the assumption of incompressibility is not too serious. The error for the birefringence is smaller since the error for thickness is smaller than that for the cross sectional area.

We assign here notations for the viscoelastic functions representing the tensile stress, σ, under uniaxial elongation at a constant rate, $\dot{\epsilon}$. The elongational viscosity growth function, η_E^+, is defined as

$$\eta_E^+(\dot{\epsilon},t) = \sigma/\dot{\epsilon} \tag{6}$$

If the function levels off with long time we obtain an elongational viscosity, η_E, as

$$\eta_E(\dot{\epsilon}) = \eta_E^+(\dot{\epsilon},\infty) \tag{7}$$

Also, we use notations η_{E0}^+ and η_{E0} to represent the limiting values at $\dot{\epsilon} \to 0$.

$$\eta_{E0}^+(t) = \eta_E^+(0,t) \tag{8}$$

$$\eta_{E0} = \eta_E(0) \tag{9}$$

Results

Stress and Birefringence. Figure 2 shows the strain dependence of the tensile stress, σ, and the birefringence, Δn, at 115 °C measured by constant-rate elongation experiments. Δn was negative over the whole strain region in this study, including the values at lower temperatures. In Figure 2, Δn is reduced with the linear stress−optical coefficient ($C = -4.7 \times 10^{-9}$ Pa^{-1}), which is valid at low stresses (σ < 2 MPa). The curves for $\Delta n/C$ should agree with σ if the SOR is valid.

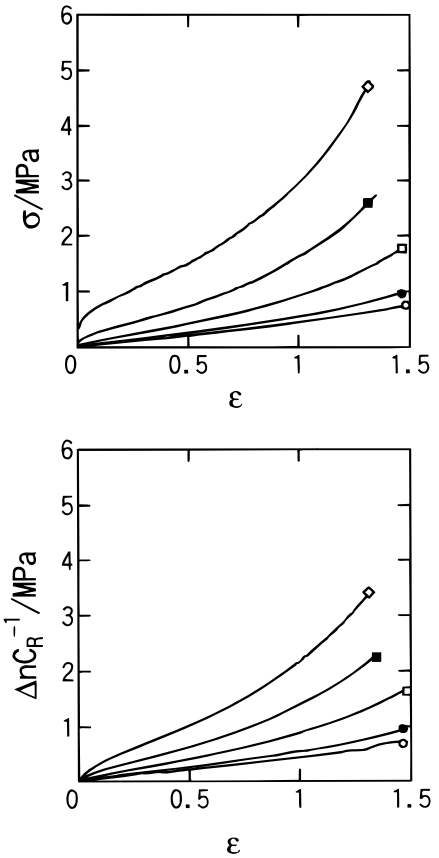

Figure 2. Strain dependence of the tensile stress, σ, and the birefringence, Δn, during constant rate elongation at 115 °C. (○) 0.0002, (●) 0.0005, (□) 0.0025, (■) 0.005, and (◇) 0.025 s^{-1}.

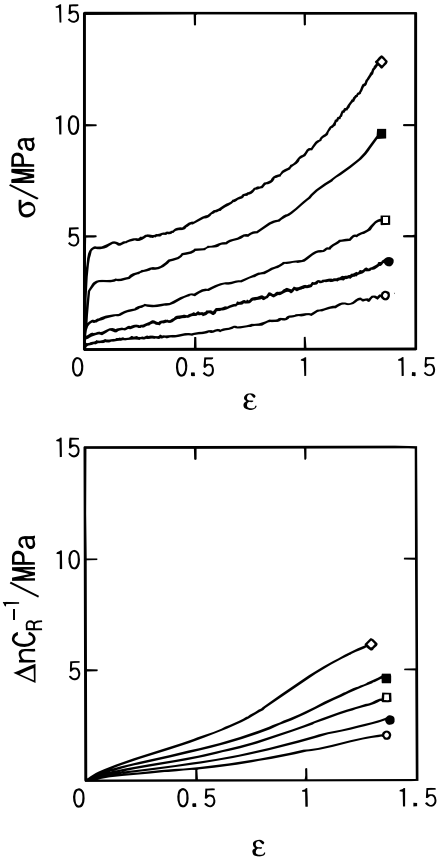

Figure 3. Strain dependence of the tensile stress, σ, and the birefringence, Δn, during constant rate elongation at 105 °C: (○) 0.00025, (●) 0.001, (□) 0.003, (■) 0.01, and (◇) 0.025 s^{-1}.

At low elongation rates ($\dot{\epsilon} = 0.0002-0.0025$ s^{-1}), the curves for $\Delta n/C$ are the same as σ. At the highest rate ($\dot{\epsilon} = 0.025$ s^{-1}), σ increases steeply at the beginning of deformation but $\Delta n/C$ does not.

The difference in strain dependence between σ and $\Delta n/C$ becomes more evident with decreasing temperatures. The data at 105 °C are shown in Figure 3. Compared with Figure 2, the strain dependence of $\Delta n/C$ is qualitatively the same while σ increases steeply at the beginning of deformation at 105 °C. This feature becomes more remarkable when the rate of elongation is increased. Similar results were obtained at 100 °C (Figure 4). At this temperature, Δn does not depend on the rate as much, while a yield phenomenon was observed for the stress variation. σ first increases, shows a maximum and a minimum, and then increases again. Thus, the variation of σ becomes complicated when the temperature approaches the glass transition temperature.

The relation between Δn and σ, which is not shown here, showed the same characteristic features as shown in Figure 1. At high temperatures and low rates, the SOR holds true. With decreasing temperatures, the stress−optical relation deviates upward from the SOR line.

Comparison with Linear Viscoelasticity. In Figure 5, the viscosity growth function, η_E^+, and $\Delta n/\dot{\epsilon}$ at 115 °C are plotted against time on the double-logarithmic scale. The dashed curve represents η_{E0}^+ calculated from the dynamic Young's modulus measured with oscillatory deformation.[14,18] This curve should agree with the curves for $\eta_E^+(\dot{\epsilon},t)$ at the limit of $\dot{\epsilon} \rightarrow 0$. Evidently, η_E^+ at various rates of elongation forms a

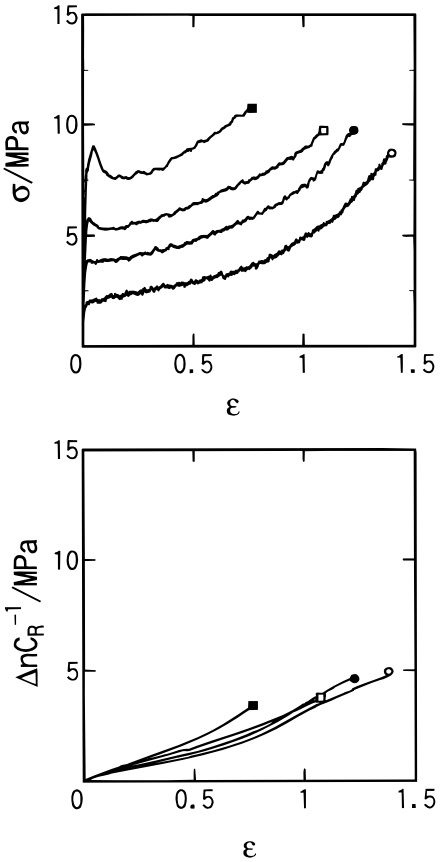

Figure 4. Strain dependence of the tensile stress, σ, and the birefringence, Δn, during constant rate elongation at 100 °C: (○) 0.0002, (●) 0.0005, (□) 0.001, and (■) 0.003 s^{-1}.

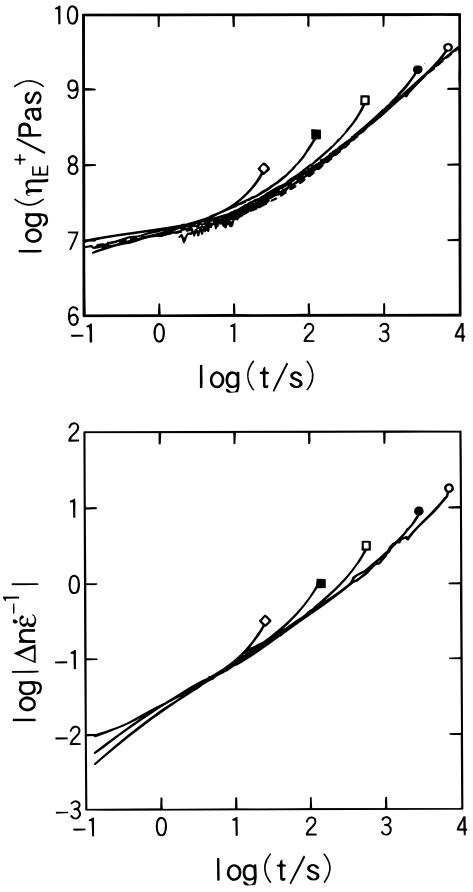

Figure 5. Viscosity growth function, η_E^+, and $\Delta n/\dot{\epsilon}$ at 115 °C. The dashed line indicates the viscosity growth function at a limit of $\dot{\epsilon} = 0$ s^{-1}.

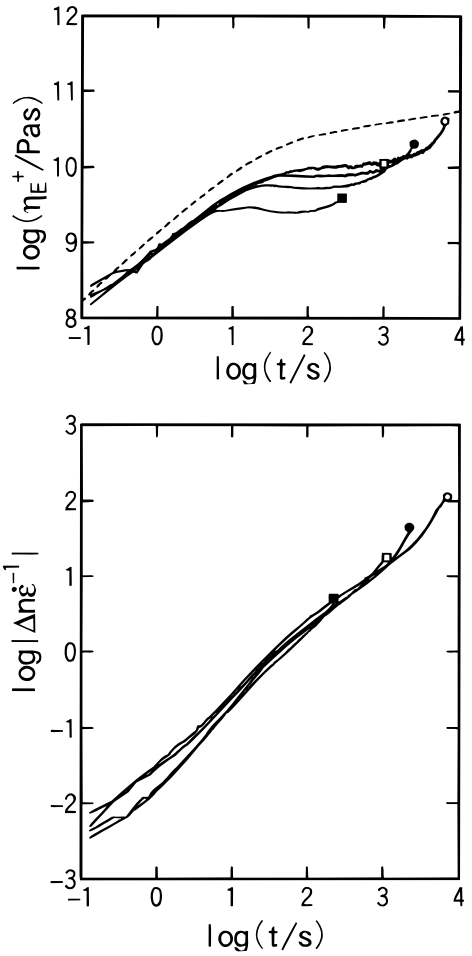

Figure 6. Viscosity growth function, η_E^+, and $\Delta n/\dot{\epsilon}$ at 100 °C. The dashed line indicates the viscosity growth function at a limit of $\dot{\epsilon} = 0$ s^{-1}.

lower envelope and this envelope agrees with η_{E0}^+ from the dynamic data. One may realize a similarity to the well-known Meissner's results for polyethylene melts,[15] but these results are for much higher stress levels. The departure of η_E^+ from the envelope begins at a certain point depending on the rate of elongation. We will discuss the origin of this divergence later. Thus, at relatively high temperatures, the stresses are approximately represented by a function η_{E0}^+ except for the steep increase of the experimental data with long times.

The time variation of $\Delta n(t)/\dot{\epsilon}$ is the same as η_E^+ with relatively long times [$\log(t/s) \geq 1$], which means that the SOR is valid. Note that the SOR is valid even after σ and Δn steeply increase. This result indicates that the steep increases observed here in σ and Δn cannot be attributed to the finite extensibility of the chain as will be discussed later. The breakdown of the SOR with short times is due to the glassy component of stress.

At lower temperatures, the results are quite different from those at a high temperature (115 °C). Figure 6 shows the time variation of η_E^+ and $\Delta n/\dot{\epsilon}$ at 100 °C. It is difficult to find any similarity to Figure 5. The dashed curves for η_{E0}^+ derived from the dynamic Young's modulus are located above the curves for η_E^+ in Figure 6. At low rates of elongation, η_E^+ increases linearly with t and then levels off once, and finally starts to diverge at a certain point. With increasing $\dot{\epsilon}$ values, the flat portion of η_E^+ curves lowers. At even the lowest $\dot{\epsilon}$, η_E^+ does not agree with η_{E0}^+. Thus, η_E^+ at the low temperatures exhibits the strong nonlinear feature of viscoelasticity even at the lowest rate of elongation studied. The curves for $\Delta n/\dot{\epsilon}$ in Figure 6 do not vary much with the rate. One may not be able to find any correlation between η_E^+ and $\Delta n/\dot{\epsilon}$ at this temperature at first glance.

Extension of the MSOR for a Highly Orientated System. According to the MSOR, the stress of molten polymers near the glass transition temperature can be separated into the two component functions as shown in eqs 2 and 3. We presume that this separation makes it easy to understand the complex features of η_E^+ and $\Delta n/\dot{\epsilon}$ of this study. The stress level is quite high for some experimental conditions, and the stress−optical coefficient for the R component should be treated as a function of the stress.[4] Muller and Pesce obtained the stress−optical relation (equilibrium curve) of PS at 120 °C when σ was less than 10 MPa by using an elongation rate $\dot{\epsilon}$ of 0.5 s^{-1}.[11] With our apparatus, such a high rate could not be achieved. However, according to their result, the stress−birefringence relation measured in the relaxation curve at lower temperatures agrees with the equilibrium curve obtained at high temperatures. Our equilibrium curve determined by this way is shown in Figure 7. Here, we performed a constant-cross-head speed experiment because the equilibrium curve can be obtained more easily than from a constant-rate experiment. This is because the relative amplitude of the G component in a constant-speed experiment decreases more rapidly due to the decrease of the rate of elongation with time. The relaxation curve forms a lower envelope, the equilibrium curve of Muller and Pesce.[11] The present curve is in good agreement with theirs. The

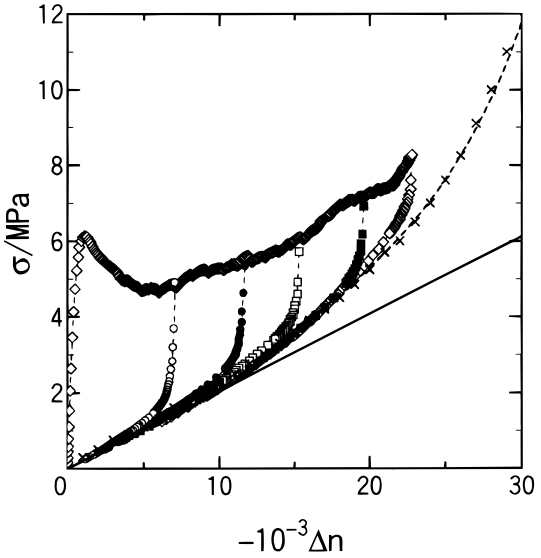

Figure 7. Stress−birefringence relation of PS during constant speed elongation ($\dot{\epsilon}_0 = 0.005$ s^{-1}) and the relaxation process after stretching to various elongation ratios, λ, at 105 °C: (○) $\lambda = 1.5$, (●) $\lambda = 2$, (□) $\lambda = 3.5$, (■) $\lambda = 3$, and (◇) $\lambda = 3.5$. The curve represents the estimated equilibrium curve (eq 12). The equilibrium curve determined by Muller and Pesce[11] is indicated by ×.

stress−optical ratio for the equilibrium curve was determined as eq 12 for $\Delta n \leq 3 \times 10^{-2}$, the range needed for later use.

Using the stress-dependent C_R, the MSOR for high stresses ($\sigma_R > 2$ MPa) may be written as follows in place of eq 3.

$$\Delta n(t) = C_R(\sigma_R)\sigma_R(t) + C_G\sigma_G(t) \quad (10)$$

The value of C_G for PS in the linear viscoelastic regime was found to be 3×10^{-12} Pa^{-1} from dynamic birefringence measurement.[9] In the following calculation, we assumed that C_G was independent of stress level. If eqs 2 and 10 are solved simultaneously, $\sigma_R(t)$ and $\sigma_G(t)$ can be determined. However, the set of eqs 2 and 10 are not convenient to solve. In a practical calculation, we treated C_R as a constant (eq 3), if the birefringence level was below 1×10^{-2}. At a higher birefringence level, the contribution of the G component to Δn may be neglected. The maximum stress measured in this study was 12 MPa, and therefore, the contribution of the $C_G\sigma_G$ term was less than 3.6×10^{-5}. Therefore, we may rewrite eq 10 as follows.

$$\Delta n(t) = C_R(\Delta n)\sigma_R(t) \ (\Delta n > 0.01) \quad (11)$$

$C_R(\Delta n)$ determined from the equilibrium curve in Figure 7 is

$$C_R/(-4.7 \times 10^{-9}\ \text{Pa}^{-1}) = 1 - 6.10(\Delta n) + (2.21 \times 10^3)(\Delta n)^2 - (6.7 \times 10^4)(\Delta n)^3 - (8.94 \times 10^5)(\Delta n)^4 + (6.8 \times 10^7)(\Delta n)^5 \quad (12)$$

Equation 12 agreed with experimental data within ±3% over the whole birefringence range. When eqs 2 and 11 are solved, the component functions, σ_R and σ_G, at high birefringence levels were obtained. In this calculation, the accuracy of σ_R is on the same order as the birefringence measurement (typically 5%). On the other hand, σ_G became less accurate with increasing strain because the relative contribution of the G component to the stress decreased.

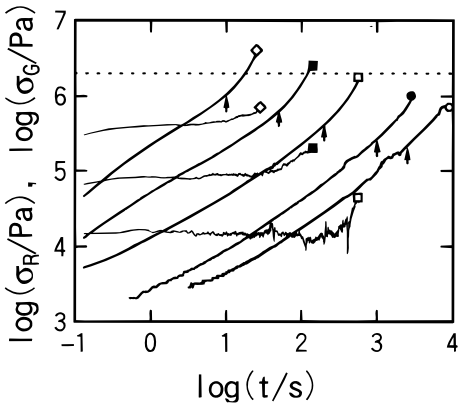

Figure 8. Two MSOR component functions at 115 °C. Arrows indicate $t = 1/(2\dot{\epsilon})$. Thick curves represent σ_R and thin curves σ_G. The dashed line indicates $\sigma = 2$ MPa over which the stress−optical coefficient, C_R, must be treated as stress-dependent.

Figure 8 shows an example of MSOR analysis: σ_R and σ_G at 115 °C are plotted against time on the double-logarithmic scale. σ_G values at $\dot{\epsilon} = 0.0002$ and 0.0005 s^{-1} were too small to be estimated accurately. σ_R increases with time, while σ_G seems to be approximately constant. The increase in σ_G with long times is due to the experimental error since the contribution of σ_G to the total stress is quite low.

Similar evaluations of σ_R and σ_G were carried out for the data at 105 and 100 °C. The results are shown in the following sections. The stress components are represented by corresponding viscosity growth functions

$$\eta_{ER}^{+}(\dot{\epsilon},t) = \sigma_R/\dot{\epsilon} \quad (13)$$

$$\eta_{EG}^{+}(\dot{\epsilon},t) = \sigma_G/\dot{\epsilon} \quad (14)$$

Effect of Elongation Rate on the R Component. Figure 9 shows the viscosity growth function, η_{ER}^{+}, of the R component. The dashed curves in Figure 9 are η_{ER0}^{+} calculated from the R component of the dynamic Young's modulus.[14] The agreement between the constant-rate experiment and dynamic measurement is good for the highest temperature, 115 °C, except with long times where η_{ER}^{+} suddenly starts to increase and deviates from linear η_{ER0}^{+} [$=\eta_{ER}^{+}(0,t)$].

Note that the divergence of η_{ER}^{+} cannot be attributed to the finite extensibility of the chain. If the finite extensibility is the reason, the σ_R values at the deviation point should coincide with each other. Moreover, at this stress level, the stress−optical relation would deviate from the linear SOR. However, this is not the case. The SOR is valid at $t > 10$ s at 115 °C in Figure 5; the upturn of the stress begins at $\sigma < 2$ MPa in Figure 8.

It is well-known that η_E diverges for a constitutive model derived from the equation of linear viscoelasticity.[16] A simple extension of the Boltzmann superposition principle for large deformation is to replace the strain with the Finger strain tensor. The elongational viscosity growth function is written as

$$\eta_E^{+}(\dot{\epsilon},t) = \frac{1}{\dot{\epsilon}}[\lambda^2(t) - \lambda^{-1}(t)]G(t) + \frac{1}{\dot{\epsilon}}\int_0^t \left[\frac{\lambda^2(t)}{\lambda^2(t')} - \frac{\lambda(t')}{\lambda(t)}\right]\mu(t-t')\mathrm{d}t \quad (15)$$

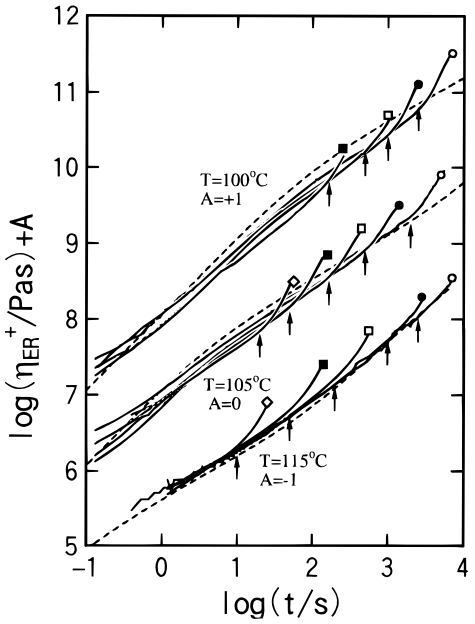

Figure 9. Viscosity growth functions for the R component, η_{ER}^+, at 115, 105, and 100 °C. The dashed curves indicate the viscosity growth functions of the R component at a limit of $\dot{\epsilon} = 0$ s^{-1}. Arrows indicate $1/(2\dot{\epsilon})$.

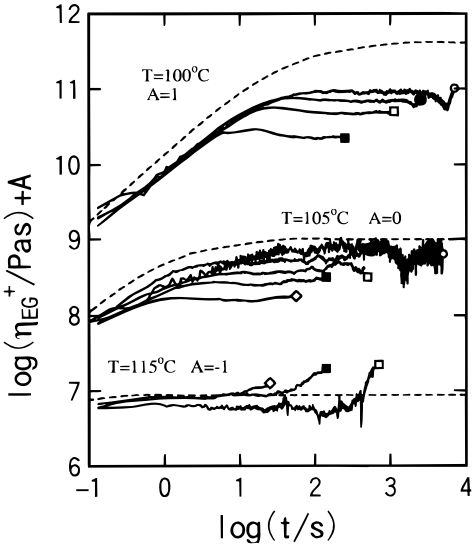

Figure 10. Viscosity growth functions for the G component, η_{EG}^+, at 115, 105, and 100 °C. The dashed curves indicate the viscosity growth functions of the G component at a limit of $\dot{\epsilon} = 0$ s^{-1} calculated from dynamic data.

where $\mu(t) = -\mathrm{d}G(t)/\mathrm{d}t$ is the memory function and $G(t)$ is the shear relaxation modulus. The elongational viscosity diverges for $\dot{\epsilon}$ values of $>1/(2\tau)$ if the memory function is represented by an exponential functions, $[\mu(t) = \exp(-t/\tau)]$. The divergence is evidently due to the rapid increase of the quantity in square brackets of eq 15 at high rates. Note that this is purely a geometrical factor arising from the choice of Finger tensor as the strain measure. The arrows in Figure 9 indicate the time t of $1/(2\dot{\epsilon})$. After time exceeds the arrows, $\eta_R^+(t)$ starts to diverge. Thus, the deviation from η_{ER}^+ can be attributed to the strong increase of strain measure.

On the other hand, if the temperature is decreased, the agreement between η_{ER}^+ and η_{ER0}^+ is not so good and η_{ER}^+ starts to depend on the rate of elongation even with short times. We will return to this point later.

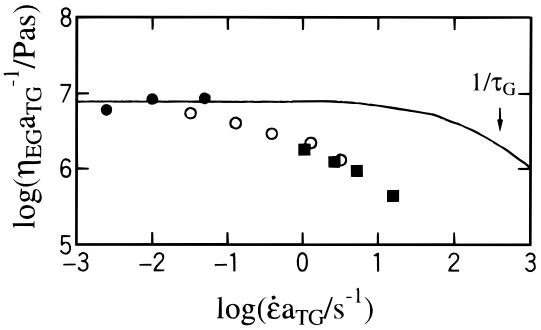

Figure 11. Rate dependence of the steady state viscosity for the G component. The reference temperature is 115 °C: (●) 115, (○) 105, and (■) 100 °C. Values of log a_{TG} are 2.1 at 105 °C and 3.7 at 100 °C. The solid line indicates $|\eta^*(t)|_{\omega=1/t}$. The arrow indicates the characteristic relaxation rate of the G component.

Effect of Elongation Rate on the G Component. Figure 10 shows the viscosity growth function for the G component, η_{EG}^+, at various temperatures. η_{EG}^+ at the limit of $\dot{\epsilon} \to 0$, η_{EG0}^+, calculated from dynamic data, is also shown for comparison. Although the system cannot reach the true steady state for the case of tensile deformation because η_{ER}^+ diverges at a finite time scale, η_{EG}^+ apparently reaches a steady state with long times and one may define the steady state viscosity, $\eta_{EG}(\dot{\epsilon})$. The data at 115 °C were not so accurate with long times as discussed previously. Neglecting these data, we can estimate the values of the steady state viscosity, $\eta_{EG}(\dot{\epsilon})$. For the highest temperature, 115 °C, these values agree with $\eta_{EG}(0)$ estimated from dynamic data.

At 105 °C, η_{EG}^+ increases with time and does not depend on $\dot{\epsilon}$ just after the beginning of deformation. With long times, η_{EG}^+ levels off and gives the steady value. The data at the lowest rate are not very far from η_{EG0}. The steady value η_{EG} decreases with increasing $\dot{\epsilon}$ values. At 100 °C, even at the lowest rate, η_{EG} did not agree with η_{EG0}. These results quite resemble the features in shear flows of the ordinary entangled polymer systems in the terminal flow zone.

Discussion

Elongation Rate Dependence of η_{EG} on $\dot{\epsilon}$. In Figure 11, the steady state viscosity η_{EG} is plotted against $\dot{\epsilon}$. Here, to compare the data at different temperatures, the data are reduced to the data at 115 °C with the method of reduced variables. η_{EG}/a_{TG} is plotted against $\dot{\epsilon}a_{TG}$, where a_{TG} is the shift factor determined by dynamic measurement.[14] The data at different temperatures lie on a single curve. Although data points are limited, this result strongly suggests that the method of reduced variables works well for the G component even in the nonlinear viscoelastic region around the glass transition zone. The figure indicates that if the rate of elongation exceeds a certain value, η_{EG} starts to decrease with increasing $\dot{\epsilon}$ values. It should be noted that this rate of elongation is about 1000 times smaller than the inverse of the characteristic relaxation time of the G component, which may be defined as $1/\omega_{max}$. Here, ω_{max} is the angular frequency at which the loss Young's modulus, $E''(\omega)$, shows a maximum in the glass-to-rubber transition zone. For the shear viscosity of polymer melts in the terminal flow zone, the rate where the thinning starts approximately corresponds to the inverse of the characteristic relaxation time. In such a case, the steady shear viscosity,

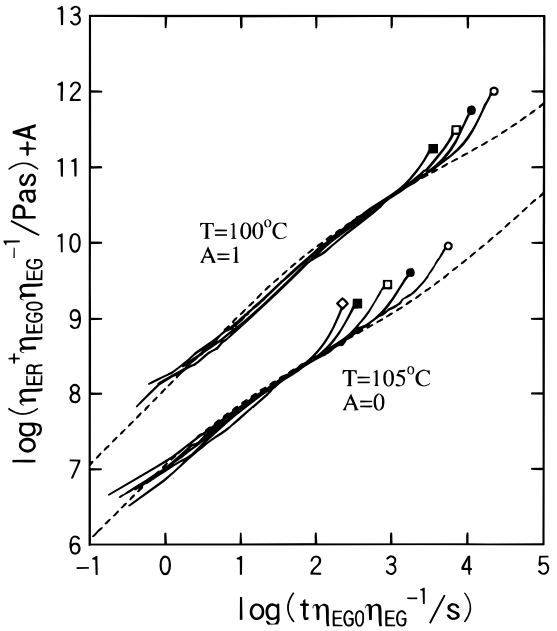

Figure 12. η_{ER}^{+} reduced by η_{EG} at 105 and 100 °C.

$\eta(\dot{\gamma})$, is close to the magnitude of the complex viscosity, $|\eta^*(\omega)|$, if the rate of shear, $\dot{\gamma}$, is equated with the angular frequency, ω.[17]

The line in Figure 11 represents $|\eta_{EG}^*(\omega)|_{\epsilon=\omega}$. This result shows that η_{EG} has a much stronger rate dependence than $|\eta_{EG}^*(\omega)|_{\epsilon=\omega}$. The shear thinning of the viscosity of polymer melts is associated with the strong strain dependence of the shear modulus.[3] The very strong rate dependence of η_{EG} may also be related to the very strong strain dependence of the Young's relaxation modulus, $E(t,\epsilon)$.[9] $E(t,\epsilon)$ for polystyrene decreases if ϵ exceeds about 1%; the structure that supports σ_G is very breakable. The remarkable yield phenomena of glassy polymers may be due to this nature of the G component. We point out that σ_G is a well-behaved viscoelastic quantity, for which the viscosity exhibits strong but smooth thinning and the method of reduced valuables works well.

Correlation between R and G Components. The curves for η_{ER}^{+} at 105 and 100 °C in Figure 9 are not as well aligned as they are at 115 °C and seem to have some systematic features. With increasing rates, the curves for η_{ER}^{+} seem to move down along a line with slope of 1 as if the temperature was being increased. Thus, the curves for η_{ER}^{+} at higher $\dot{\epsilon}$ values deviates more and more from that for η_{ER0}^{+} (dashed curve) in contrast to the case of 115 °C where η_{ER}^{+} completely agreed with η_{ER0}^{+} except for the upturn at the end.

Here, we discuss the correlation between the R and the G component. As discussed before, η_{EG} shows the strong thinning phenomenon at lower temperatures. If the G component represents the properties of an effective medium with viscosity η_{EG} in which the chain orientation relaxes, the relaxation rate of the R component may be accelerated by decreasing η_{EG}. To examine this conjecture, the η_{ER}^{+} was reduced using η_{EG}. A reduced function, $\eta_{ER}^{+}(\eta_{EG0}/\eta_{EG})$, is plotted against a reduced time, $t(\eta_{EG0}/\eta_{EG})$. The results are shown in Figure 12. The agreement among different rates becomes much better. Also, the reduced curve lies fairly close to the dashed curve representing η_{ER0}^{+} except with long times. Thus, the deviation of η_{ER} from the prediction of linear viscoelasticity can well be attributed to the decrease of effective viscosity due to thinning of the G component.

Conclusion

We have examined the viscoelastic properties of polystyrene under large deformations just above the glass transition temperature. The strain−stress relation can be more easily understood if the stress is separated into the two component functions by using the modified stress−optical rule, including the nonlinear stress dependence of the stress−optical coefficient. The glassy component (G) shows strong strain rate dependence if the deformation rate exceeds about $^1/_{1000}$ of its characteristic relaxation time. On the other hand, the behavior of the R component, which is related to chain orientation, can be explained in the framework of linear viscoelasticity except for the enhanced relaxation rate at high rates of strain when the temperature is close to the glass transition temperature. This means that the effective friction coefficient for the R component may be controlled by the state of the surrounding medium which can be probed by viscoelastic response of the G component.

Acknowledgment. The PS sample was kindly supplied by Mitsui Toatsu Co. Ltd. This study was partially supported by a Grant-in-Aid for Scientific Research (09450361) from the Ministry of Education, Science and Culture of Japan.

References and Notes

(1) Janeschitz-Kriegl, H. *Polymer Melt Rheology and Flow Birefringence*; Springer-Verlag: Berlin, 1983.
(2) Doi, M.; Edwards, S. F. *The Theory of Polymer Dynamics*; Clarendon: Oxford, 1986.
(3) Larson, R. G. *Constitutive Equations for Polymer Melts and Solutions*; Butterworth: Sydney, 1988.
(4) Matsumoto, T.; Bogue, D. C. *J. Polym. Sci., Polym. Phys. Ed.* **1977**, *15*, 1663.
(5) Inoue, T.; Okamoto, H.; Osaki, K. *Macromolecules* **1991**, *24*, 5670.
(6) Osaki, K.; Okamoto, H.; Inoue, T.; Hwang, E.-J. *Macromolecules* **1995**, *28*, 3625.
(7) Inoue, T.; Okamoto, H.; Mizukami, Y.; Matsui, H.; Watanabe, H.; Kanaya, T.; Osaki, K. *Macromolecules* **1996**, *29*, 6240.
(8) Inoue, T.; Matsui, H.; Murakami, S.; Kojiya, S.; Osaki, K. *Polymer* **1997**, *38*, 1215.
(9) Okamoto, H.; Inoue, T.; Osaki, K. *Macromolecules* **1992**, *25*, 3413.
(10) Inoue, T.; Okamoto, H.; Osaki, K. *Macromolecules* **1992**, *25*, 7069.
(11) Muller, R.; Pesce, J. J. *Polymer* **1994**, *35*, 734.
(12) Treloar, L. R. G. *The Physics of Rubber Elasticity*; Clarendon: Oxford, 1958.
(13) Kimura, S.; Osaki, K.; Kurata, M. *J. Polym. Sci., Polym. Phys. Ed.* **1981**, *19*, 151.
(14) Inoue, T.; Hayashihara, H.; Okamoto, H.; Osaki, K. *J. Polym. Sci., Polym. Phys. Ed.* **1992**, *30*, 409.
(15) Meissner, J. *J. Appl. Polym. Sci.* **1972**, *16*, 2877.
(16) Chang, H.; Lodge, A. S. *Rheol. Acta* **1972**, *11*, 127.
(17) Cox, W. P.; Merz, E. H. *J. Polym. Sci.* **1958**, *28*, 619.
(18) Since the complex Young's modulus, $E^*(\omega)$, is not thermorheologically simple around the glass transition temperature, the master curve of $E^*(\omega)$ at 115, 105, and 100 °C was first calculated following the method described in ref *14*. The master curve of $E^*(\omega)$ at each temperature was reconstructed from the master curves of the component functions and shift factors for them. Then $\eta_E^{+}(t)$ was calculated from $E^*(\omega)$ using the relation of linear viscoelasticity.

MA970908I